Behavioral/Systems/Cognitive

Modulation of Circuit Feedback Specifies Motor Circuit Output

Dawn M. Blitz[1,2] **and Michael P. Nusbaum**[1]

[1]Department of Neuroscience, Perelman School of Medicine, University of Pennsylvania, Philadelphia, Pennsylvania 19104-6074, and [2]Department of Zoology, Miami University, Oxford, Ohio 45056

Bidirectional communication (i.e., feedforward and feedback pathways) between functional levels is common in neural systems, but in most systems little is known regarding the function and modifiability of the feedback pathway. We are exploring this issue in the crab (*Cancer borealis*) stomatogastric nervous system by examining bidirectional communication between projection neurons and their target central pattern generator (CPG) circuit neurons. Specifically, we addressed the question of whether the peptidergic post-oesophageal commissure (POC) neurons trigger a specific gastric mill (chewing) motor pattern in the stomatogastric ganglion solely by activating projection neurons, or by additionally altering the strength of CPG feedback to these projection neurons. The POC-triggered gastric mill rhythm is shaped by feedback inhibition onto projection neurons from a CPG neuron. Here, we establish that POC stimulation triggers a long-lasting enhancement of feedback-mediated IPSC/Ps in the projection neurons, which persists for the same duration as POC-gastric mill rhythms. This strengthened CPG feedback appears to result from presynaptic modulation, because it also occurs in other projection neurons whose activity does not change after POC stimulation. To determine the function of this strengthened feedback synapse, we compared the influence of dynamic-clamp-injected feedback IPSPs of pre- and post-POC amplitude into a pivotal projection neuron after POC stimulation. Only the post-POC amplitude IPSPs elicited the POC-triggered activity pattern in this projection neuron and enabled full expression of the POC-gastric mill rhythm. Thus, the strength of CPG feedback to projection neurons is modifiable and can be instrumental to motor pattern selection.

Introduction

Feedback from neural circuits to their inputs is common in neural systems (Sillito et al., 2006; Briggs and Usrey, 2008; Bonjean et al., 2011; Ego-Stengel et al., 2012). However, whether this feedback is subject to modulation and, if so, what function it serves is unknown in most systems. In rhythmic motor systems, the activity of projection neuron inputs to central pattern generator (CPG) circuits is commonly regulated by rhythmic synaptic feedback from the activated CPG (Gillette et al., 1978; Arshavsky et al., 1988; Dubuc and Grillner, 1989; Nagy et al., 1994; Frost and Katz, 1996; Norris et al., 1996; Ezure and Tanaka, 1997; Blitz and Nusbaum, 2008; Buchanan and Einum, 2008). This rhythmic feedback causes the projection neuron activity pattern to be time-locked to the CPG-generated motor pattern. The function of this feedback and the associated rhythmic activity pattern in the projection neurons is unknown in most systems. Thus far, this feedback enables intercircuit regulation (Bartos et al., 1999; Wood et al., 2004; Blitz and Nusbaum, 2008), and it prolongs projection neuron activity and consequently activation of the target CPG (Antri et al., 2009).

Many aspects of rhythmic motor systems are subject to neuromodulation, which configures different CPG outputs and helps select the projection neurons that drive CPG activity (Dickinson, 2006; Doi and Ramirez, 2008; Jordan and Sławińska, 2011; Nusbaum and Blitz, 2012). Despite the common presence of CPG feedback to projection neurons, it remains to be determined whether this feedback is also under modulatory control. Therefore, we are using the crab gastric mill (chewing) system to determine whether CPG feedback inhibition of identified projection neurons is modulated by an identified peptidergic input. Specifically, we are examining whether the post-oesophageal commissure (POC) neurons modulate the strength of the inhibitory feedback synapse from the gastric mill and pyloric (food filtering) CPG interneuron anterior burster (AB) onto the projection neurons modulatory commissural neuron 1 (MCN1) and commissural projection neuron 2 (CPN2) and, if so, what function it serves.

The POC neurons trigger a long-lasting activation of MCN1 and CPN2 in the commissural ganglion (CoG), thereby eliciting a gastric mill rhythm in the stomatogastric ganglion (STG) (Blitz et al., 2008). The POC-triggered gastric mill motor pattern is distinct from other gastric mill motor patterns, notably in the pyloric-timed activity pattern of the projection- and protractor phase CPG neurons (Blitz et al., 2008; White and Nusbaum, 2011).

Here, we establish that the AB feedback synapse onto MCN1 and CPN2 is strengthened after POC stimulation, likely via a

Received March 18, 2012; revised May 14, 2012; accepted May 14, 2012.

Author contributions: D.M.B. and M.P.N. designed research; D.M.B. performed research; D.M.B. and M.P.N. analyzed data; D.M.B. and M.P.N. wrote the paper.

This work was supported by National Institute of Neurological Disorders and Stroke Grant R37-NS29436 (M.P.N.) and National Science Foundation Grant IOS-1153417 (D.M.B.). We thank Wolfgang Stein for assistance with data analysis and stimulation protocols, Michael Hughes (Statistical Consulting Center, Miami University) for advice on statistical analysis, and Farzan Nadim for assistance with the dynamic-clamp model AB.

Correspondence should be addressed to Dr. Dawn M. Blitz, 242 Pearson Hall, Department of Zoology, Miami University, Oxford, OH 45056. E-mail: dawn.blitz@muohio.edu.

DOI:10.1523/JNEUROSCI.1461-12.2012

 0270-6474/12/329182-12$15.00/0

presynaptic modulation of AB transmitter release. We then use dynamic-clamp manipulations to show that POC modulation of this feedback synapse is necessary to enable the projection neurons and, consequently, a gastric mill CPG neuron to exhibit the pyloric-timed activity that characterizes the POC-gastric mill rhythm. Thus, CPG feedback regulation of projection neuron activity is subject to modulation, which in turn shapes the CPG-generated motor pattern.

Materials and Methods

Animals. Male *Cancer borealis* crabs were obtained from commercial suppliers (Yankee Lobster Company; Marine Biological Laboratory) and maintained in commercial tanks containing recirculating, filtered, and aerated artificial seawater (10°C) before use. Before dissection, crabs were cold anesthetized by packing in ice for at least 30–40 min. The stomatogastric nervous system (STNS) was dissected as described previously (Blitz et al., 2004; Gutierrez and Grashow, 2009). Briefly, the foregut was removed and pinned ventral side up in a Sylgard 170 (K.R. Anderson; World Precision Instruments)-coated glass bowl, in chilled (9–12°C) *C. borealis* saline. The *poc* (see Fig. 1) was visualized with a dissecting microscope and bisected, after which the stomach was bisected ventrally and pinned flat, dorsal side up. The STNS, including all four ganglia plus their connecting and peripheral nerves (see Fig. 1), was then freed from surrounding tissue, removed from the surface of the foregut, and pinned down in a Sylgard 184 (K.R. Anderson; World Precision Instruments)-coated Petri dish. The isolated STNS was maintained in chilled (9–12°C) saline that was continually superfused (7–12 ml/min) across the preparation throughout the subsequent experiment.

Solutions. C. borealis saline included the following (in mM): 440 NaCl, 26 $MgCl_2$, 13 $CaCl_2$, 11 KCl, 10 Trizma base, 5 maleic acid, and 5 dextrose, pH 7.4–7.6.

Electrophysiology. Extracellular recordings were obtained by placing one of a pair of stainless-steel wires inside the main bath compartment and the other wire alongside a small region of nerve that was isolated with petroleum jelly (Vaseline; Medical Accessories and Supply Headquarters). Loose-patch recordings were made by applying suction through a glass electrode placed near axons in the desheathed superior oesophageal nerve (*son*) (see Fig. 1). Extracellular nerve recordings and axonal loose-patch recordings were amplified using A-M Systems model 1700 AC amplifiers and Brownlee Precision model 410 amplifiers.

Intracellular recordings were obtained using sharp glass microelectrodes, made from borosilicate glass, filled with 0.6 M K_2SO_4 plus 10 mM KCl (15–25 MΩ) or 4.0 M K-acetate plus 35 mM KCl (15–25 MΩ). Intracellular signals were amplified using Axoclamp 2B and 900A amplifiers (Molecular Devices) in bridge mode, discontinuous current-clamp mode (3–10 kHz sampling rate), or discontinuous single-electrode voltage-clamp mode (3–15 kHz sampling rate) and digitized at ~5 kHz using a Micro 1401 data acquisition interface and Spike2 software (Cambridge Electronic Design). To facilitate intracellular electrode placement, ganglia were desheathed and viewed with light transmitted through a dark-field condenser (Nikon). STG circuit neurons and CoG projection neurons were identified based on their activity patterns, synaptic connectivity, and extracellularly recorded axonal projection patterns (Weimann et al., 1991; Beenhakker and Nusbaum, 2004; Saideman et al., 2007).

POC-gastric mill rhythms, lasting ~5–30 min, were triggered by extracellular stimulation of one or both halves of the bisected *poc* (tonic stimulation, 15–30 Hz; duration, 30 s) (Blitz and Nusbaum, 2008; Blitz et al., 2008). To test the impact of different gastric mill rhythm-related MCN1 activity patterns on the activity of the gastric mill CPG neuron lateral gastric (LG), we used playback of MCN1 activity recorded under three conditions, including during natural AB feedback, pre-POC and post-POC amplitude dynamic-clamp AB input (see below). We used each of these three patterns to stimulate the inferior oesophageal nerve (*ion*) at a voltage that selectively activates the MCN1 axon (Coleman and Nusbaum, 1994; Bartos and Nusbaum, 1997). For these experiments, we removed the CoGs by bisecting the *ions* and *sons*. Under these conditions, the played back MCN1 activity was not time-locked to the ongoing pyloric rhythm in the STG. Thus, to eliminate the presence of two uncoordinated sources of pyloric-timed input to the gastric mill circuit, we suppressed the pyloric rhythm in the STG by injecting hyperpolarizing current into the PD neurons. The cycle period of gastric mill rhythms driven by pyloric-timed MCN1 activity is not significantly different with the pyloric rhythm on versus off (Wood et al., 2004).

Dynamic clamp. AB activity was modeled in dynamic-clamp software (http://cancer.rutgers.edu/software/index.html) to mimic natural AB activity (~1 Hz cycle period; 6 spikes per burst; ~200 ms burst duration) (Marder and Eisen, 1984b; Blitz and Nusbaum, 2008). After measuring the pre-POC amplitude of AB inhibition in MCN1, AB was hyperpolarized to suppress the natural AB inhibition, and the dynamic-clamp version of this synaptic action was tuned to match the natural AB inhibition in each preparation. Specifically, in each experiment, the maximal conductance of the dynamic-clamp AB inhibition was adjusted to match the natural inhibition amplitude in MCN1. After POC stimulation, dynamic-clamp AB inhibition was injected into MCN1 at both the control amplitude and at a twofold to threefold higher maximal conductance, based on the average increase in the peak IPSC amplitude (see Results). We set the reversal potential at −80 mV based on voltage-clamp recordings in MCN1 (see Results), and the voltage dependence and time constants of activation and inactivation of the dynamic-clamp synaptic currents were hand-tuned to mimic the properties of natural AB synaptic currents (Blitz and Nusbaum, 2008; this study).

Data analysis. Data analysis was performed using Spike2 (Cambridge Electronic Design), IGOR Pro (WaveMetrics), and Excel (Microsoft) software. IPSC area was calculated by subtracting the baseline holding current and measuring the area in a 200–400 ms epoch beginning at the start of AB/PD activity. IPSC/P peaks were measured from the baseline current/voltage to the peak of the last AB-mediated IPSC/P in each AB burst. To measure the time course of modulation of IPSC area, 10 cycles were averaged before POC stimulation and at several time points relative to the end of POC stimulation. The number of AB action potentials per pyloric-timed burst was measured from loose-patch recordings in the *son*, to eliminate the possibility of an impalement-induced change in spike number. Firing frequency was measured as the number of action potentials per burst minus one, divided by the burst duration. Input resistance was determined by injecting steps of current (+0.5 to −1.0 nA; 600 ms duration) from a baseline that was more negative than action potential threshold and dividing each average (5–10 steps) steady-state voltage change by the current amplitude.

To quantify the extent of pyloric-timed activity in MCN1, CPN2, and LG, we determined the percentage of action potentials that occurred within each bin out of the total number of spikes across the normalized pyloric cycle (50 bins per pyloric cycle). The pyloric cycle was measured as the duration between the onset of two consecutive PD neuron bursts (Bucher et al., 2006). To compare the impact of natural AB and dynamic-clamp AB inhibition on spiking, we calculated the area under the curve for the percentage of total spikes occurring during the initial 0–0.35 of the normalized pyloric cycle. This region of the cycle was selected based on MCN1 and CPN2 activity being inhibited on average for the first 35% of the normalized pyloric cycle during the POC-gastric mill rhythm (Blitz et al., 2008). The area under the curve was measured as the area under a line connecting the height of each bin from 0 to 0.35 of the pyloric cycle for each preparation under each condition. Statistical analysis was then performed by comparing this region across conditions. All data reported are the average of at least 10 consecutive pyloric cycles. Figures were made using Spike2, IGOR, and CorelDraw (Corel Corporation).

Statistical tests, including the paired Student's *t* test, Spearman's correlation, and one-way repeated-measures ANOVA (RM ANOVA) followed by Tukey's *post hoc* analysis, were used as indicated. Significance was considered to be $p < 0.05$. Data are expressed as mean ± SE. Statistical significance was assessed with SigmaStat (Systat Software).

Results

The POC neurons are a bilateral population of ~100 peptidergic [*C. borealis* tachykinin-related peptide Ia (CabTRP Ia)] neurons per side that innervate the CoGs via the circumoesophageal commissures (*cocs*) and *poc* (Fig. 1*A*) (Blitz et al., 2008). These neu-

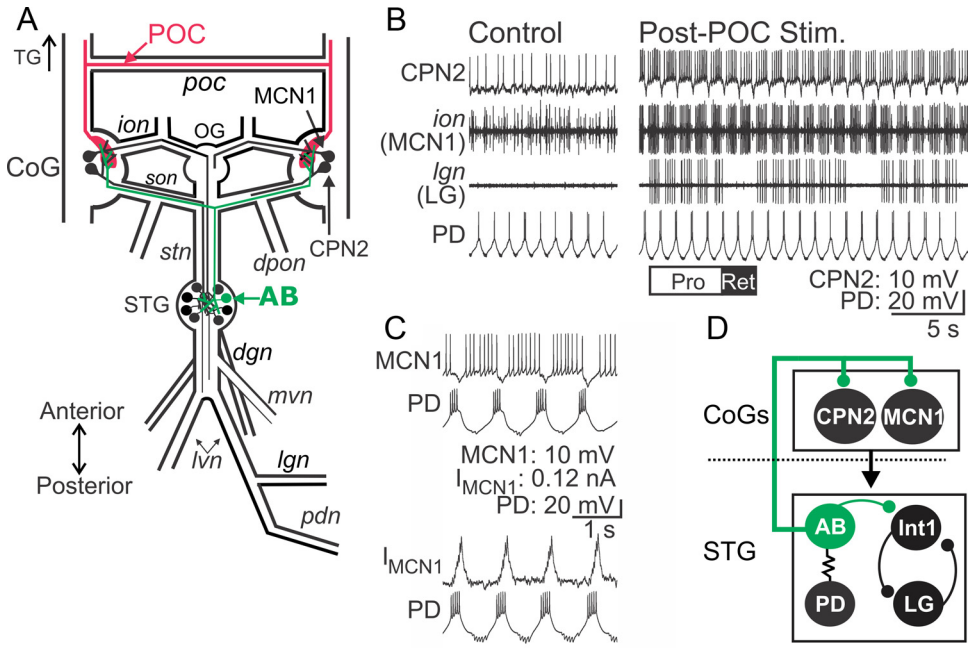

Figure 1. POC neurons activate MCN1 and CPN2 to trigger a particular version of the gastric mill rhythm. ***A***, Schematic of the STNS illustrating the axon pathways of projection (MCN1, CPN2), CPG feedback (AB), and extrinsic input (POC) neurons. There is a single MCN1 and CPN2 in each CoG, ~100 POC axons entering each CoG, and a single AB neuron in the STG. For clarity, the complete axonal pathways of MCN1 and CPN2 are only illustrated unilaterally. Abbreviations: Ganglia: CoG, Commissural ganglion; OG, oesophageal ganglion; STG, stomatogastric ganglion. Nerves: *dgn*, dorsal gastric nerve; *dpon*, dorsal posterior oesophageal nerve; *ion*, inferior oesophageal nerve; *lgn*, lateral gastric nerve; *lvn*, lateral ventricular nerve; *mvn*, medial ventricular nerve; *pdn*, pyloric dilator nerve; *poc*, post-oesophageal commissure; *son*, superior oesophageal nerve; *stn*, stomatogastric nerve. Neurons: AB, anterior burster; CPN2, commissural projection neuron 2; MCN1, modulatory commissural neuron 1; POC, post-oesophageal commissure. ***B***, Left, During control conditions, MCN1 and CPN2 are weakly active, there is an ongoing pyloric rhythm (PD neuron) and there is no gastric mill rhythm (LG neuron silent in the *lgn* recording). Right, POC stimulation triggers a gastric mill rhythm that is characterized by rhythmic interruptions in the activity of MCN1, CPN2, and the gastric mill protractor motor neuron LG that are time-locked to the ongoing pyloric rhythm (e.g., PD neuron) (Blitz et al., 2008). The white ("PRO") and black ("RET") bars indicate protraction and retraction phases of one cycle of the gastric mill rhythm. ***C***, Pyloric (PD neuron)-timed inhibition is evident in a MCN1 recording as barrages of IPSPs that transiently eliminate MCN1 activity (top) and IPSCs in voltage-clamp recording mode (bottom). MCN1 recordings in both panels are from the same preparation. ***D***, Schematic highlighting the feedback inhibitory synapse from AB onto MCN1 and CPN2 in the CoGs (Blitz and Nusbaum, 2008). The AB soma is in the STG, from which it projects an axon to innervate each CoG and cause glutamatergic inhibition of projection neurons, including MCN1 and CPN2 (Blitz and Nusbaum, 1999). The dotted line indicates spatial separation of the CoGs from the STG. AB is electrically coupled to both PD neurons, causing them to fire during the same phase of the pyloric rhythm (Marder and Eisen, 1984a). Thus, activity of the more readily accessible PD neuron is often used as a marker of AB activity.

rons do not extend axons past the CoGs and therefore do not innervate the STG (Blitz et al., 2008). Brief (15–30 s) POC stimulation triggers a long-lasting (5–20 min) activation of the CoG projection neurons MCN1 and CPN2, which in turn drive the gastric mill rhythm in the STG (Fig. 1*B*) (Blitz and Nusbaum, 2008; Blitz et al., 2008; White and Nusbaum, 2011). The gastric mill rhythm is a two-phase motor pattern (protraction, retraction) that controls the chewing movements of the teeth within the gastric mill stomach compartment (Heinzel et al., 1993; Hedrich et al., 2011).

The POC version of the gastric mill rhythm is distinguished by the pyloric rhythm-timed activity pattern of the projection neurons MCN1 and CPN2 as well as the gastric mill CPG neuron LG during protraction (Fig. 1*B*,*C*) (Blitz et al., 2008; White and Nusbaum, 2011). During other versions of the gastric mill rhythm, LG, MCN1, and CPN2 instead fire tonically during protraction (Beenhakker et al., 2004; Blitz et al., 2004; Christie et al., 2004; Saideman et al., 2007). The core rhythm generator for the POC-gastric mill rhythm includes the reciprocally inhibitory protractor motor neuron LG and retractor interneuron Int1 (Fig. 1*D*) (White and Nusbaum, 2011).

The pyloric rhythm influence on the gastric mill motor pattern results primarily from the influence of the pyloric pacemaker interneuron AB, via its inhibitory synapses onto several gastric mill neurons in the STG and onto MCN1 and CPN2 in the CoGs (Fig. 1*C*,*D*) (Bartos et al., 1999; Blitz and Nusbaum, 2008; White and Nusbaum, 2011). The pyloric rhythm, which is also generated in the STG, has a cycle period (~1 s) that is ~10 times briefer than the gastric mill cycle period (~10 s) (Fig. 1*B*,*C*) (Marder and Bucher, 2007).

The pyloric-timed LG burst pattern results from POC stimulation triggering a long-lasting, pyloric-timed activity pattern in MCN1 and CPN2, which they then impose via synaptic actions onto LG (Fig. 1*B–D*) (Blitz and Nusbaum, 2008; Blitz et al., 2008). As done previously (Blitz and Nusbaum, 2008), we often recorded the paired pyloric dilator (PD) motor neurons activity to represent the timing of AB activity. PD neuron recordings are more accessible than AB recordings, and these three neurons are electrically coupled and fire their pyloric-timed bursts during the same pyloric phase (Fig. 1*D*) (Eisen and Marder, 1982; Miller and Selverston, 1982a,b; Marder and Bucher, 2007).

POC neurons strengthen CPG feedback inhibition onto MCN1 and CPN2

In parallel with POC stimulation eliciting pyloric-timed activity in MCN1 and CPN2, previous studies suggested that the amplitude of the AB inhibition in these projection neurons increased after POC stimulation (Blitz et al., 2008). We aimed to determine whether this was indeed the case and, if so, determine whether it contributed to defining the POC-gastric mill motor pattern. We first performed a voltage-clamp analysis to determine whether POC stimulation modulated the magnitude of this inhibitory action. As illustrated in Figures 1*C* and 2, each burst of AB action potentials elicits a barrage of summating IPSCs in MCN1 and

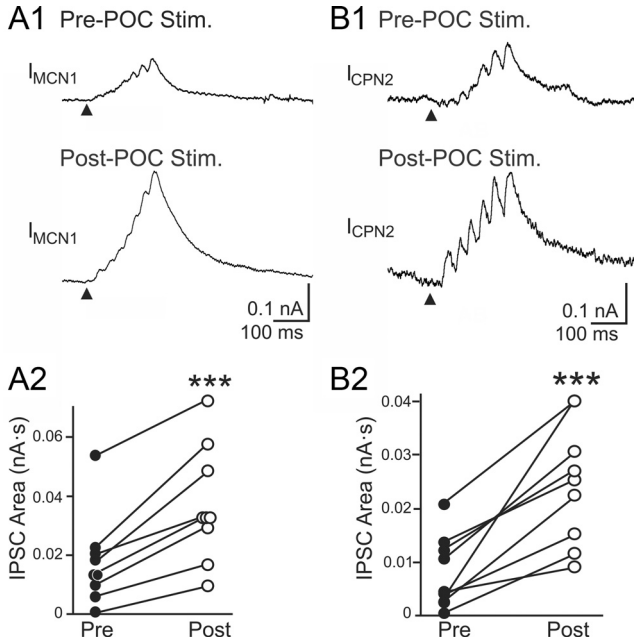

Figure 2. POC stimulation triggers an increased AB IPSC area in MCN1 and CPN2. Average IPSC barrage in MCN1 (***A1***) and CPN2 (***B1***) is shown before and after POC stimulation. Fifty AB bursts were averaged for MCN1, and 10–13 AB bursts were averaged for CPN2. The arrowheads indicate onset of AB/PD activity. Recordings in ***A*** and ***B*** are from separate preparations. ***A2***, ***B2***, The average area of the AB-mediated IPSC barrage per preparation in MCN1 ($n = 9$) (***A2***) and CPN2 ($n = 9$) (***B2***) is plotted before and after POC stimulation. Each line connects the corresponding data points for a single preparation. $^{***}p < 0.001$.

CPN2 (Blitz and Nusbaum, 2008). To quantify these inhibitory events, we measured the area of each IPSC barrage using a holding potential between −60 and −70 mV. The control value for these barrages in MCN1 was 0.017 ± 0.005 nA · s ($n = 9$), while in CPN2 it was 0.008 ± 0.002 nA · s ($n = 9$). POC stimulation triggered an increase in the AB-mediated IPSC area in both MCN1 (0.037 ± 0.006 nA · s; $n = 9$; $p = 0.0001$, paired t test) and CPN2 (0.025 ± 0.004 nA · s; $n = 9$; $p = 0.0007$, paired t test) (Fig. 2). These increases in the AB-mediated IPSC area after POC stimulation occurred in every preparation (Fig. 2).

We next aimed to determine the functional consequences of this enhanced feedback inhibition. Under baseline *in vitro* conditions, MCN1 and CPN2 are weakly active or silent (Figs. 1*B*, 3*A*,*B*) and this activity level does not elicit a gastric mill rhythm (Beenhakker and Nusbaum, 2004; Blitz et al., 2008). At these times, both neurons consistently exhibited small (0.5–5 mV: 2.36 ± 0.38 mV; $n = 11$) or minimal (<0.5 mV: 0.21 ± 0.05 mV; $n = 6$) pyloric-timed hyperpolarizations (Fig. 3*A*,*B*). This was the case despite the fact that there was always an ongoing, vigorous pyloric rhythm (cycle period, 0.98 ± 0.04 s; $n = 17$).

The small-amplitude pyloric-timed hyperpolarizations in MCN1 and CPN2 before POC stimulation might have resulted from a limited driving force, due to the projection neuron resting potentials being relatively close to the reversal potential for the AB-mediated IPSPs (MCN1 V_{rest}, −64.5 ± 2.6 mV, $n = 9$; CPN2 V_{rest}, −55.7 ± 2.8 mV, $n = 8$). Additionally, both MCN1 and CPN2 exhibit a long-lasting depolarization (to approximately −40 mV) after POC stimulation, which increases the driving force on the AB-mediated IPSPs. Thus, to better evaluate the effectiveness of the AB inhibition onto these projection neurons under control conditions relative to its effectiveness after POC stimulation, we injected depolarizing current into these neurons under baseline conditions to move them to a potential (approximately −40 mV) comparable to their depolarized phase after POC stimulation (Figs. 1*B*, 3*A*,*B*). Despite the increased driving force on the AB-mediated IPSPs after MCN1 and CPN2 were depolarized by current injection, AB inhibition of these projection neurons still appeared to be smaller in amplitude and less effective relative to its influence after POC stimulation (Fig. 3*A*,*B*).

To quantify the extent to which AB inhibition interrupted MCN1 and CPN2 spiking, we determined the timing of MCN1 and CPN2 action potentials relative to the normalized pyloric cycle (Fig. 3*C*). We then quantified the area under the curve of these plots from each preparation during 0.0–0.35 of the normalized pyloric cycle (see Materials and Methods). After POC stimulation, the percentage of spikes occurring during the initial 35% of the normalized pyloric cycle was reduced for both MCN1 and CPN2, compared with the percentage of spikes occurring during this portion of the pyloric cycle before POC stimulation (MCN1, $p = 0.033$; CPN2, $p = 0.045$; $n = 4$ each; paired t test) (Fig. 3*C*). The AB-mediated inhibition more effectively reduced spiking in MCN1 and CPN2 after POC stimulation despite these neurons exhibiting an equivalent (CPN2) or higher (MCN1) firing frequency after POC stimulation relative to their pre-POC firing rate at −40 mV (MCN1: pre-POC, 17.1 ± 1.9 Hz; post-POC, 30.7 ± 1.5 Hz; $n = 4$; $p = 0.01$, paired t test) (CPN2: pre-POC, 11.0 ± 3.4 Hz; post-POC, 26.9 ± 7.5 Hz; $n = 4$; $p = 0.05$, paired t test).

Likely presynaptic enhancement of AB feedback inhibition to MCN1 and CPN2 by POC stimulation

There are multiple mechanisms that might underlie the increased AB-mediated IPSC area in MCN1/CPN2 after POC stimulation. For example, this might have resulted from increased AB neuron activity. Although the direct POC actions are confined to the CoGs (Blitz et al., 2008), the increased MCN1 activity triggered by POC stimulation increases AB activity when the initial AB activity is sufficiently weak (Bartos and Nusbaum, 1997) (M. P. Nusbaum and D. M. Blitz, unpublished observations). To test whether increased AB activity contributed to the increased AB-mediated IPSC area in MCN1/CPN2, we determined whether there was a change in the number of AB action potentials per pyloric-timed burst and/or its firing frequency. Before POC stimulation, there was no gastric mill rhythm. After POC stimulation, AB activity was quantified separately during the protraction and retraction phases of the POC-triggered gastric mill rhythm. This separate analysis was performed because, during a different version of the gastric mill rhythm that also involves MCN1, several pyloric rhythm parameters are distinct during the gastric mill protraction and retraction phases (Bartos and Nusbaum, 1997). Here, however, after POC stimulation there was no change in AB activity during gastric mill protraction or retraction relative to before POC stimulation (Fig. 4) (spikes per burst: $p = 0.72$, one-way RM ANOVA, $n = 3$; firing frequency: $p = 0.43$, one-way RM ANOVA, $n = 3$).

The lack of change in AB activity after POC stimulation suggested that there was no change in AB actions within the STG, despite the observed change at the AB synapses onto MCN1 and CPN2 in the CoGs (Fig. 2). The strengthened inhibitory action of AB onto MCN1 and CPN2 therefore likely resulted from a direct POC action at these synapses, which could have occurred presynaptically and/or postsynaptically. In support of a postsynaptic locus, at the MCN1 and CPN2 resting potentials POC stimulation elicited an increased input resistance (R_{input}) in MCN1 (pre-

POC, 20.6 ± 2.4 MΩ; post-POC, 25.8 ± 2.4 MΩ; $p = 0.01$, paired t test; $n = 6$), although not in CPN2 (33.2 ± 9.1 to 43.1 ± 11.0; $p = 0.095$, paired t test; $n = 4$).

In addition to the fact that there was not a significant change in the CPN2 input resistance after POC stimulation, we expected that a postsynaptic POC action would comparably increase R_{input} and IPSC amplitude. However, the mean percentage increase in the peak AB IPSC amplitude in MCN1 and CPN2 after POC stimulation was considerably larger than the mean percentage increase in their R_{input} (IPSC, 320 ± 106%; R_{input}, 42 ± 14%, $n = 6$; $p = 0.04$, paired t test). Furthermore, there was no correlation between the change in peak IPSC and the change in R_{input} triggered by POC stimulation (change in IPSC amplitude, 0.13 ± 0.04 nA; change in R_{input}, 10.0 ± 2.3 MΩ; $p > 0.05$, Spearman's correlation; $n = 6$). The fact that the voltage-clamp data in Figure 2 were obtained at holding potentials comparable to those at which the input resistance measurements were obtained provided additional support for the hypothesis that any postsynaptic contribution was likely to be minor. It was also unlikely that a POC-independent increased input resistance occurs upon depolarization in MCN1 and CPN2, which thereby contributed to the increased AB inhibition when these neurons are depolarized by POC stimulation. For example, as shown in Figure 3, the AB inhibition of MCN1 and CPN2 was smaller before POC stimulation when they were depolarized to the same membrane potential to which they were depolarized after POC stimulation.

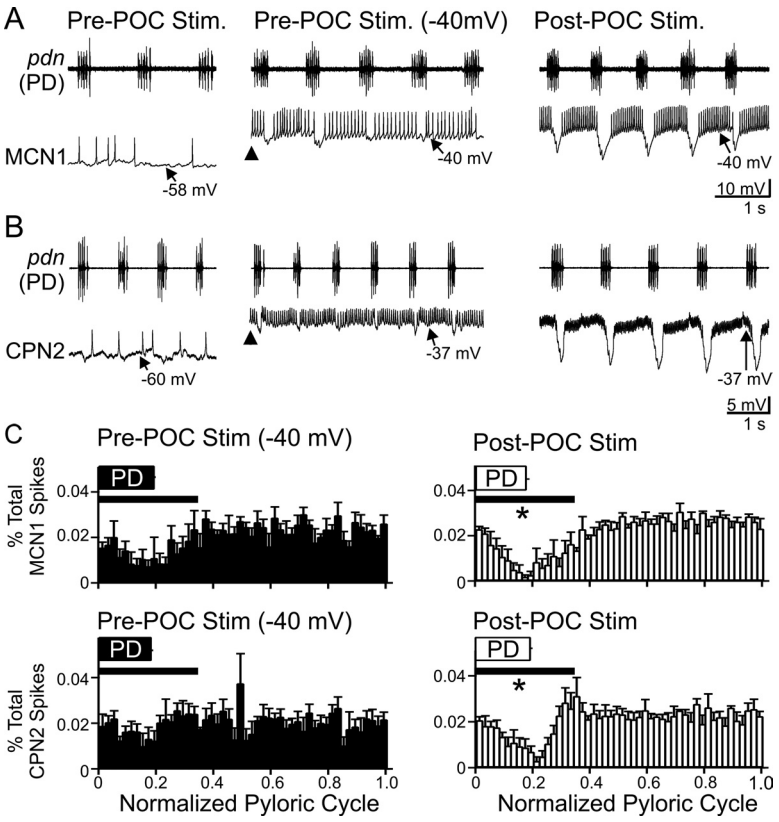

Figure 3. CPG feedback to projection neurons is strengthened by POC stimulation. ***A***, ***B***, Left, At their resting potentials before POC stimulation, AB inhibition is weak in MCN1 and CPN2. Middle, Before POC stimulation, MCN1 and CPN2 were depolarized via intracellular current injection to approximately −40 mV (arrowheads). Under this condition, AB inhibition elicits small-amplitude hyperpolarizations in MCN1 and CPN2 that modestly regulate their firing rate. Right, POC stimulation depolarizes MCN1 and CPN2 to approximately −40 mV, during which time AB inhibition elicits larger amplitude hyperpolarizations and longer duration pauses in their firing, despite their firing rate being increased (MCN1) or comparable (CPN2) relative to their activity during the current injections before POC stimulation (see Results). MCN1 and CPN2 recordings are from different preparations. ***C***, The percentage of MCN1 (top) and CPN2 (bottom) action potentials per bin (2% of pyloric cycle per bin) and the phase of AB/PD activity (PD box) are plotted against the normalized pyloric cycle (see Materials and Methods) before (left) and after (right) POC stimulation. The pre-POC stimulation data were obtained while MCN1/CPN2 was depolarized by continual current injection to approximately −40 mV. After POC stimulation, there is a larger decrease in the percentage of MCN1/CPN2 spikes during the initial 35% of the normalized pyloric cycle (bar), relative to pre-POC stimulation. Means ± SEM per bin are plotted. MCN1: $n = 4$; CPN2: $n = 4$. $^*p < 0.05$.

To examine whether there was a presynaptic component to the POC modulation of the AB-mediated IPSC in MCN1 and CPN2, we measured AB inhibition in other CoG projection neurons that exhibit no long-term response to POC stimulation. We focused on the identified projection neurons MCN5 and MCN7, which also influence the STG motor circuits and receive AB feedback (Norris et al., 1996; Blitz et al., 1999; Blitz and Nusbaum, 2008). Although MCN5 was transiently excited during POC stimulation ($n = 5$) and MCN7 was briefly excited after POC stimulation ($n = 5$), there was no lasting change in their activity (Fig. 5). Consequently, during the time after POC stimulation when MCN1 and CPN2 were activated and driving the gastric mill rhythm, MCN5 and MCN7 firing rates were not different from their prestimulation levels (MCN5: $p = 0.31$; MCN7: $p = 0.45$, paired t test; $n = 5$ each) (Fig. 5). There was also no change in the MCN5 input resistance after POC stimulation (pre-POC: 23.3 ± 5.7 MΩ; post-POC: 27.6 ± 8.6 MΩ; $p = 0.25$, paired t test; $n = 4$). Nonetheless, AB inhibition of both neurons was increased after POC stimulation (MCN7 IPSP peak amplitude: pre-POC, 1.1 ± 0.2 mV; post-POC, 2.9 ± 0.7 mV, $n = 5$; $p = 0.03$, paired t test; MCN5 IPSC area: pre-POC, 0.06 ± 0.02 nA · s; post-POC, 0.10 ± 0.01 nA · s; $p = 0.04$, paired t test; $n = 4$) (Fig. 5). Thus, all four recorded CoG projection neurons exhibited an increased inhibitory input from AB after POC stimulation, despite the fact that the activity of two of them (MCN5, MCN7) was unchanged by that stimulation. This supported the hypothesis that the POC neurons trigger a presynaptic enhancement of the AB feedback inhibition to CoG projection neurons, likely by selectively increasing transmitter release from the CoG terminals of the AB neuron.

POC enhancement of CPG feedback is pivotal to the POC-gastric mill motor pattern

We hypothesized that the POC-triggered enhancement of the AB feedback was necessary for generation of the POC-gastric mill motor pattern. If that was indeed the case, the enhancement of the feedback synapse should have persisted for a duration similar to that of the POC-triggered motor pattern (see above) (Blitz et al., 2008). To determine whether this was the case, we measured the AB-mediated IPSC area in MCN1 before and at several time points after POC stimulation. Relative to the pre-POC stimulation time point, this IPSC area was increased from the first time

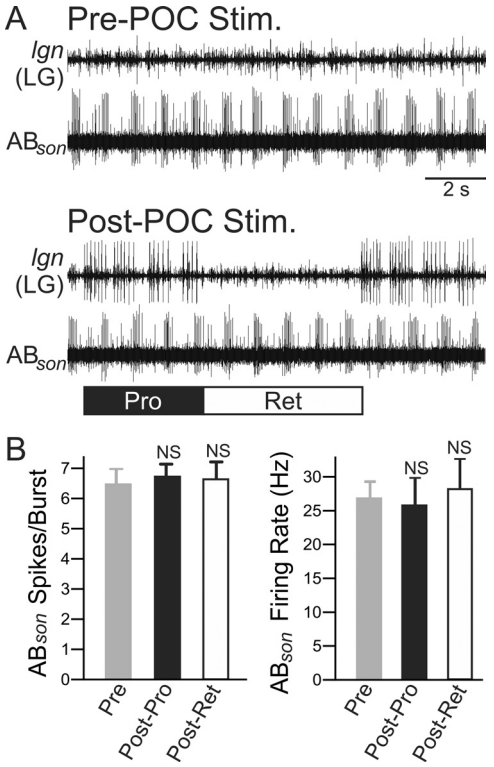

Figure 4. POC stimulation does not trigger a change in AB activity. ***A***, Suction electrode recordings from the AB axon in the *son* illustrate that the activity of AB appears similar pre- and post-POC stimulation. Before POC stimulation, there was no gastric mill rhythm (no LG activity in *lgn*), but there was a pyloric rhythm (rhythmic AB bursting). Note that POC stimulation triggered a gastric mill rhythm, represented by the LG neuron bursting (*lgn*), but did not evidently change AB firing rate or burst duration. ***B***, Quantification of the average number of action potentials per pyloric-timed AB burst (left) and AB intraburst firing frequency (right) indicate no difference between pre- and post-POC stimulation. After POC stimulation, AB activity was quantified separately during the protraction (Post-Pro) and retraction (Post-Ret) phases of the gastric mill rhythm. Error bars indicate SEM. NS, $p > 0.05$.

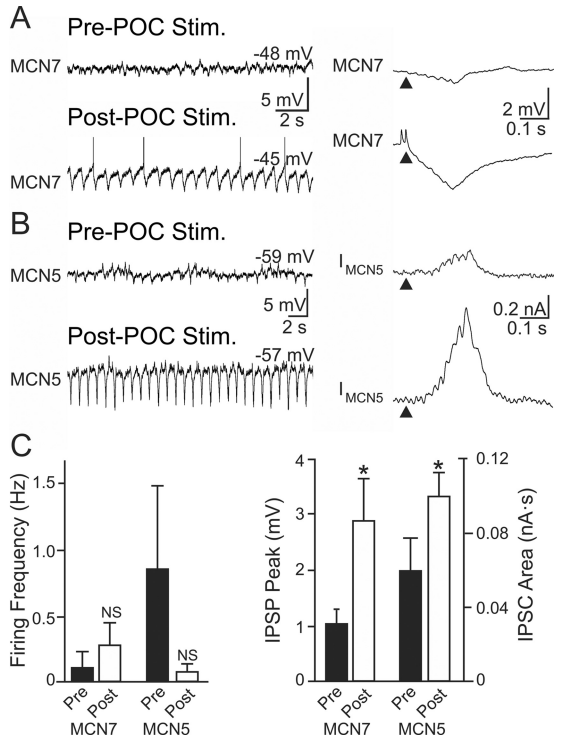

Figure 5. POC stimulation triggers increased AB IPSP/C amplitude in nonactivated CoG projection neurons. ***A***, ***B***, Left, The activity of the CoG projection neurons MCN7 (***A***) and MCN5 (***B***) is not altered after POC stimulation. Right, However, the average AB-mediated IPSP amplitude in MCN7 (10 cycles) and IPSC amplitude in MCN5 (20 cycles) increases after POC stimulation. ***C***, There was no change in MCN7 or MCN5 firing frequency after POC stimulation. However, the AB-mediated IPSP amplitude measured in MCN7 and IPSC area measured in MCN5 both increased after POC stimulation. Error bars indicate SEM. *$p < 0.05$; NS, $p > 0.05$.

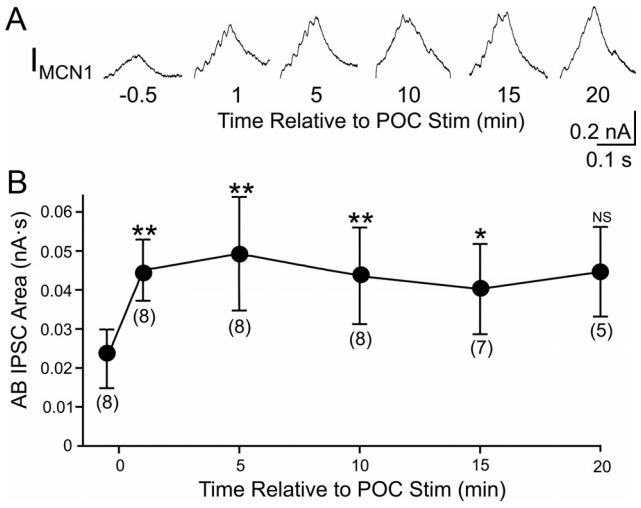

Figure 6. The POC modulation of AB feedback to CoG projection neurons is long-lasting. ***A***, Average traces (10 cycles/trace) of AB IPSCs in MCN1 at several time points relative to POC stimulation. ***B***, The AB IPSC area is plotted against time relative to POC stimulation. Numbers in brackets indicate the number of preparations contributing to each data point. Error bars indicate SEM. **$p < 0.01$; *$p < 0.05$; NS, $p > 0.05$.

point tested (60 s) after POC stimulation through the 15 min time point (Fig. 6). The mean IPSC area value for the 20 min time point appeared comparable with the 15 min time point but was not significantly different from the pre-POC condition ($p = 0.05$), possibly due to the lower n value for the 20 min time point ($n = 5$; earlier time points: $n = 7–8$) (Fig. 6). Thus, the POC-triggered enhancement of the AB inhibition persisted for a time frame that was similar to that for the POC-triggered gastric mill motor pattern, suggesting a role in specifying the POC version of this motor pattern.

We next aimed to determine the functional consequences of this long-lasting enhanced AB feedback inhibition of MCN1 and CPN2 during the POC-gastric mill rhythm. We first tested, separately, the necessity of MCN1 and CPN2 for eliciting a POC-gastric mill rhythm. Previous work showed that selectively stimulating MCN1 in a pyloric-timed pattern is sufficient to drive a POC-like gastric mill rhythm (Wood et al., 2004). Supporting this previous study, suppressing MCN1 activity with a voltage-clamp holding potential of −70 mV eliminated an ongoing POC-gastric mill rhythm in all five preparations tested. In contrast, a comparable suppression of CPN2 activity altered but did not eliminate the gastric mill rhythm ($n = 4$). Because only MCN1 activity was necessary to drive the POC-gastric mill rhythm, we focused on it to study the functional consequences of the POC-enhanced AB feedback inhibition onto the projection neurons.

To test the functional relevance of the POC-triggered enhancement of the AB feedback to MCN1, we used dynamic-clamp-simulated AB feedback so that the relative impact of its pre- and post-POC amplitude could be examined after POC stimulation (Fig. 7). After the POC neurons were stimulated and

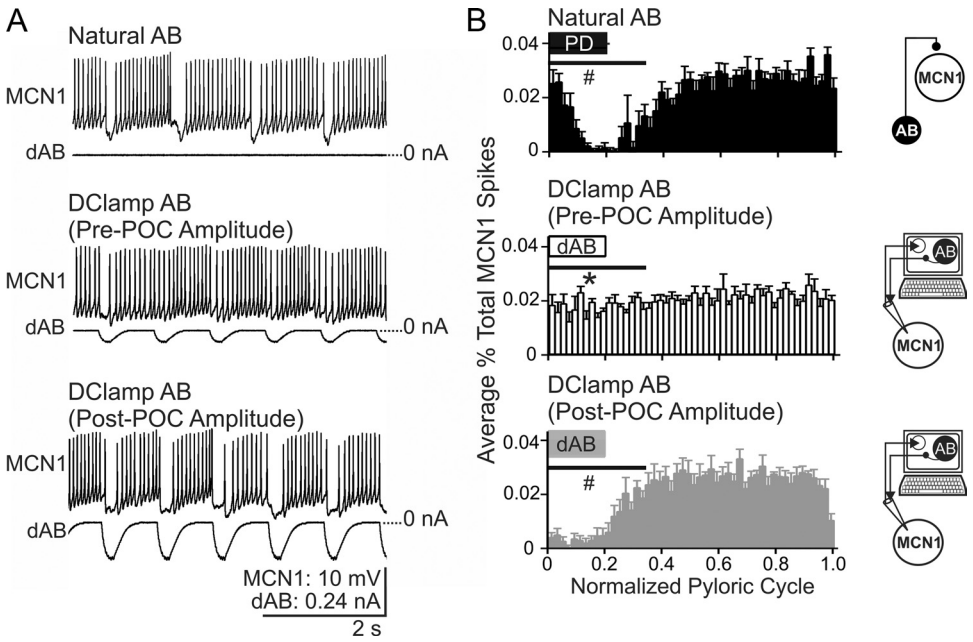

Figure 7. The pre-POC stimulation amplitude of AB inhibition is not sufficient to elicit pyloric-timed activity in MCN1 after POC stimulation. ***A***, After POC stimulation, natural AB inhibition suppresses MCN1 activity, resulting in a pyloric-timed MCN1 firing pattern. Replacing the natural AB inhibition of MCN1 with dynamic-clamp AB (dAB) inhibition injected at the pre-POC amplitude is not sufficient to reliably suppress MCN1 firing, although it does modulate the MCN1 firing frequency. Using the post-POC amplitude, dAB inhibition injected into MCN1 does successfully suppress MCN1 firing, causing pyloric-timed MCN1 activity similar to that occurring in response to natural AB inhibition. ***B***, The percentage of MCN1 action potentials per bin and the phase of AB/PD activity (box) are plotted against the normalized pyloric cycle for three conditions: natural AB inhibition of MCN1, plus pre- and post-POC amplitude dAB inhibition of MCN1. In response to natural AB inhibition and post-POC amplitude dAB inhibition, there is a decrease in the percentage of MCN1 spikes occurring during the initial 35% of the normalized pyloric cycle relative to pre-POC dAB inhibition. The effect of dAB inhibition begins earlier in the normalized pyloric cycle than the natural AB inhibition because there is only a brief delay (~5 ms) from the onset of the dAB burst in the dynamic-clamp software to the injection of dAB inhibition into MCN1. In contrast, there is a conduction delay of ~25 ms for the natural AB spikes to travel from the STG to each CoG (Blitz and Nusbaum, 2008). The horizontal bars indicate the region of statistical analysis. Schematics to the right of each panel indicate whether natural AB inhibition was present or dAB inhibition was injected into MCN1. The arrows indicate that MCN1 voltage is read into, and dAB current is sent out from the dynamic-clamp software. Error bars indicate SEM. $^{*}p < 0.05$ compared with natural AB; $^{\#}p < 0.05$ compared with pre-POC dAB.

the MCN1 activity was recorded with natural AB synaptic input, the AB feedback was eliminated (by hyperpolarizing current injection into the PD neurons) and dynamic-clamp AB inhibition was injected into MCN1 at both the control and modulated amplitude. The control amplitude in each experiment was injected using a maximal conductance in the dynamic-clamp software that elicited IPSPs that matched the natural AB IPSP amplitude before POC stimulation (i.e., "pre-POC amplitude") (see Materials and Methods). To mimic the post-POC modulated amplitude, we used a maximal conductance that was twofold to threefold greater than the maximal conductance used to mimic the control amplitude in each experiment. This value was based on the average increase in the peak IPSC amplitude (see above) elicited by POC stimulation. The reversal potential of the dynamic-clamp AB inhibition was based on the reversal potential of AB IPSCs measured in MCN1 (-86.8 ± 4.5 mV; $n = 3$).

After POC stimulation, with the pyloric rhythm active, MCN1 activity was interrupted during each rhythmic AB/PD burst (Figs. 1*B*,*C*, 3*A*,*C*, 7). When natural AB activity was suppressed and replaced with a dynamic-clamp version of its inhibitory input to MCN1 at the pre-POC amplitude, each rhythmic dynamic-clamp AB burst tended to weaken but not terminate MCN1 firing (Fig. 7*A*). In contrast, when the amplitude of dynamic-clamp AB inhibition was increased to match the post-POC amplitude of the natural AB inhibition, MCN1 activity was interrupted during each AB burst, matching the effect of the natural AB (Fig. 7*A*).

We quantified the impact of the AB inhibition on MCN1 activity by measuring the MCN1 spike distribution during the normalized pyloric cycle, as in Figure 3*C*. The percentage of MCN1 action potentials occurring during the initial 35% of the pyloric cycle, measured as the area under the curve (see Materials and Methods), was not different in response to natural AB inhibition and post-POC amplitude dynamic-clamp inhibition (one-way RM ANOVA, Tukey's test, $p > 0.05$; $n = 5$) (Fig. 7*B*). Under both conditions, MCN1 activity was consistently interrupted by the natural or artificial AB inhibition. In contrast, there was a greater percentage of MCN1 action potentials overlapping with AB/PD activity in response to the pre-POC amplitude dynamic-clamp inhibition, compared with natural AB inhibition and post-POC amplitude dynamic-clamp inhibition (one-way RM ANOVA, Tukey's test, $p < 0.05$; $n = 5$) (Fig. 7*B*). Thus, after POC stimulation, the control amplitude of AB inhibition did not consistently interrupt MCN1 activity and configure it into a pyloric-timed pattern.

To determine the consequences of the enhanced AB inhibition of MCN1 for the POC-triggered gastric mill motor pattern, we characterized the activity pattern of the gastric mill CPG neuron LG when MCN1 was stimulated using each of the MCN1 activity patterns from the manipulations shown in Figure 7. Specifically, we drove MCN1 activity using the MCN1 patterns recorded after POC stimulation during natural AB feedback, dynamic-clamp injection of the pre-POC amplitude AB inhibition, and dynamic-clamp injection of post-POC amplitude inhibition (see Materials and Methods). These three MCN1 patterns enabled us to assess the impact of differences in the strength of AB feedback to MCN1 on the LG activity pattern.

Playback of the MCN1 activity pattern recorded in the presence of natural AB feedback elicited a gastric mill rhythm in

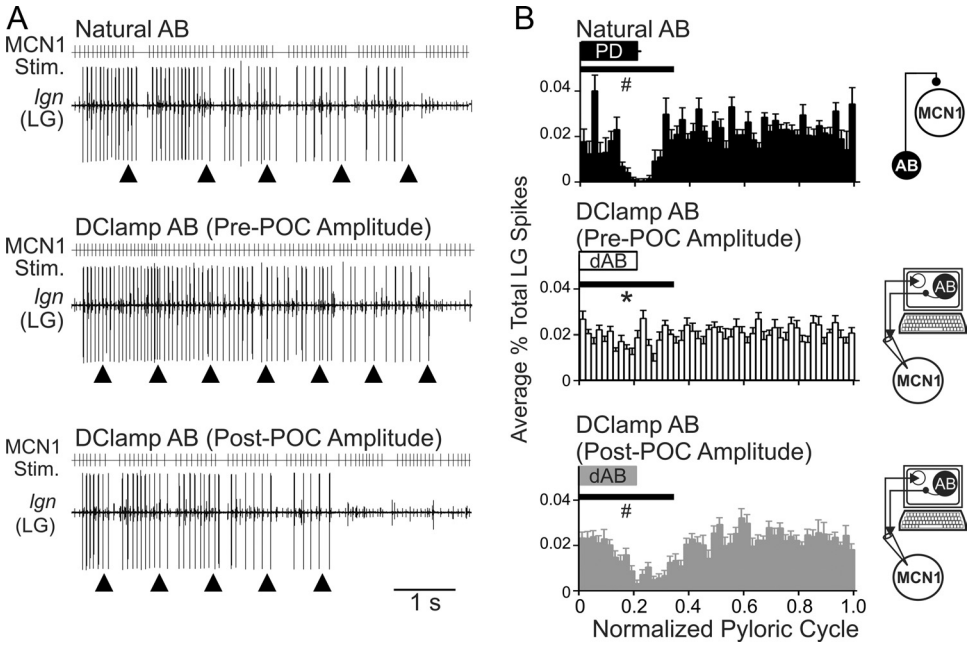

Figure 8. POC-modulation of the AB feedback synapse to MCN1 is necessary for the POC-triggered gastric mill motor pattern. ***A***, MCN1 was stimulated (MCN1 Stim.) using the activity patterns recorded in response to natural AB feedback (top), pre-POC amplitude dAB (middle), and post-POC amplitude dAB (bottom) (see Materials and Methods). The pre-POC amplitude dynamic-clamp stimulation pattern did not elicit pyloric-timed interruptions in the LG bursts, whereas the other two conditions did elicit pyloric-timed pauses in LG firing such as are characteristic of the POC-gastric mill rhythm. The arrowheads indicate onset of natural or dynamic-clamp AB activity. ***B***, The average percentage of LG action potentials per bin and the phase of AB/PD activity are plotted against the normalized pyloric cycle for three conditions: top, natural AB; middle, pre-POC amplitude dAB; bottom, post-POC amplitude dAB. MCN1 stimulation patterns based on the MCN1 activity pattern during natural AB inhibition and post-POC amplitude dAB inhibition resulted in a smaller percentage of LG spikes during the initial 35% of the normalized pyloric cycle, relative to the MCN1 pattern occurring during the pre-POC amplitude dAB inhibition. The horizontal bars indicate the region of statistical analysis. Schematics to the right of each panel indicate whether natural AB inhibition was present or dAB inhibition was injected into MCN1. The arrows are as in Figure 7. Error bars indicate SEM. $^{*}p < 0.05$ compared with natural AB; $^{\#}p < 0.05$ compared with pre-POC dAB.

which the LG neuron consistently exhibited pyloric-timed pauses in its burst (Fig. 8*A*). This pattern was comparable with the LG pattern occurring during the natural POC-gastric mill rhythm (Fig. 1*B*). In contrast, when we used the MCN1 activity pattern recorded during pre-POC amplitude dynamic-clamp AB inhibition, a gastric mill rhythm was consistently elicited but the LG burst structure exhibited considerably fewer and briefer pauses during the AB inhibition ($n = 9$) (Fig. 8*A*). When we instead stimulated MCN1 using its pattern in response to the post-POC amplitude dynamic-clamp AB inhibition, the LG activity pattern was comparable to that occurring with the natural MCN1 pattern ($n = 9$) (Fig. 8*A*).

We quantified the LG response to each of the aforementioned MCN1 stimulation patterns by determining the percentage of LG action potentials per bin across the normalized pyloric cycle, with particular attention to the AB/PD burst period, as done for the MCN1 analysis in Figure 7*B*. Stimulating MCN1 with the pattern recorded in response to pre-POC amplitude dynamic-clamp AB inhibition resulted in consistently more LG action potentials overlapping with the AB burst compared with using the MCN1 pattern that occurred during natural AB feedback or in response to the post-POC amplitude dynamic-clamp AB inhibition ($p < 0.05$, one-way RM ANOVA, Tukey's test; $n = 9$) (Fig. 8*B*). This result supported the hypothesis that the POC-triggered MCN1 activity pattern that occurred during the pre-POC amplitude AB inhibition was unable to drive LG in the POC pattern. In contrast, the POC-triggered MCN1 activity pattern resulting from post-POC amplitude AB inhibition elicited an LG firing pattern that was comparable with the LG pattern elicited by natural AB feedback inhibition ($p > 0.05$, one-way RM ANOVA, Tukey's test; $n = 9$) (Fig. 8*B*). Thus, POC activation of MCN1 is sufficient to trigger a gastric mill rhythm, even in the presence of the pre-POC AB feedback synapse, which is too weak to consistently regulate the MCN1 activity pattern. However, the full expression of the POC version of the gastric mill rhythm, in which the LG firing pattern exhibits pyloric-timed pauses (Blitz et al., 2008; White and Nusbaum, 2011; this study), required the POC-enhanced AB feedback synapse.

Changing the MCN1 activity pattern from rhythmic to tonic alters other aspects of the gastric mill motor pattern in addition to the LG burst structure (Wood et al., 2004). Thus, we examined whether other parameters of the POC-gastric mill rhythm also depended on the enhanced AB inhibition of MCN1. Using the same experiments as in Figure 8, we quantified the gastric mill cycle period and number of LG action potentials per burst. With respect to cycle period, the gastric mill rhythm was slower when driven by the POC-triggered MCN1 activity pattern resulting from pre-POC amplitude dynamic-clamp AB inhibition compared with either natural AB inhibition (one-way RM ANOVA, Tukey's test, $p < 0.05$; $n = 9$) or post-POC amplitude dynamic-clamp inhibition ($p < 0.05$; $n = 9$). There was no difference in cycle period between the natural AB inhibition and post-POC amplitude dynamic-clamp inhibition conditions ($p > 0.05$; $n = 9$). Similarly, more LG action potentials per protractor phase occurred during gastric mill rhythms driven by the POC-triggered MCN1 activity pattern resulting from pre-POC amplitude dynamic-clamp AB inhibition relative to rhythms driven by MCN1 patterns elicited by both natural AB inhibition (one-way RM ANOVA, Tukey's test, $p < 0.05$; $n = 9$) and post-POC amplitude AB inhibition ($p < 0.05$; $n = 9$). There was no difference in the number of LG spikes per burst during gastric mill rhythms driven by the POC-triggered MCN1 activity pattern resulting

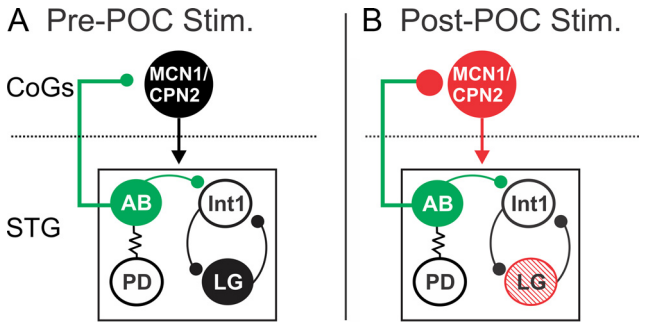

Figure 9. POC stimulation triggers a specific version of the gastric mill rhythm via postsynaptic activation of MCN1 and CPN2 and presynaptic modulation of the AB feedback synapse to these projection neurons. ***A***, Before POC stimulation, AB inhibition of MCN1 and CPN2 is weak, plus the projection neurons and LG are weakly active or silent and there is no gastric mill rhythm (black circles). ***B***, POC stimulation triggers a long-lasting activation of MCN1 and CPN2 (red) that includes a pyloric rhythm-timed activity pattern due to a long-lasting strengthening of the AB inhibition of these projection neurons (red) without a change in AB activity (green). Note that there is not a concomitant strengthening of AB inhibition within the STG (green). The presynaptic and postsynaptic POC actions on MCN1 and CPN2 are both necessary for the POC version of the gastric mill rhythm, which is characterized by pyloric-timed activity patterns in the projection neurons and the protraction neuron LG (red stripes). The dotted line indicates spatial separation of the CoGs from the STG.

from natural AB inhibition and post-POC amplitude dynamic-clamp inhibition ($p > 0.05$; $n = 9$).

Discussion

In this paper, we demonstrate that the ability of a modulatory input to trigger a particular rhythmic motor pattern requires its modulation of a CPG feedback synapse onto the projection neurons that drive the CPG. This presynaptic modulation of the CPG feedback synapse occurs in parallel with the direct postsynaptic modulatory excitation of the projection neurons (Fig. 9). Specifically, in the crab STNS, the peptidergic POC neurons strengthen the inhibitory feedback synapse from the CPG neuron AB onto the projection neurons MCN1 and CPN2, in parallel with the direct POC excitation of these two projection neurons. The strengthened feedback synapse is necessary to enable the appropriate MCN1 activity pattern, which in turn drives the canonical POC-triggered gastric mill motor pattern (Fig. 9) (Blitz and Nusbaum, 2008; Blitz et al., 2008; White and Nusbaum, 2011). Although we did not determine the function played by POC strengthening of the feedback synapse onto CPN2, the resulting pyloric-timed CPN2 activity likely contributes to the pyloric-timed activity in the gastric mill protractor neurons (LG, GM neurons) that are excited by CPN2 during the POC-rhythm (Norris et al., 1994; Beenhakker and Nusbaum, 2004; Blitz et al., 2008). These same protractor neurons fire tonic bursts during other gastric mill motor patterns (Beenhakker and Nusbaum, 2004; Blitz et al., 2004; Christie et al., 2004).

Our results support the hypothesis that the phase-locking of MCN1 and CPN2 to the pyloric rhythm following POC stimulation results from a long-term presynaptic modulation of the AB_{CoG} synapses. This presynaptic modulation of AB_{CoG} may well result from the POC neurons release of the peptide CabTRP Ia, which these neurons contain and use in the CoGs to cause a long-lasting excitation of MCN1 and CPN2 (Blitz et al., 2008). This hypothesis is supported by the observation that brief CabTRP Ia pressure ejection near the MCN1 and CPN2 CoG arborizations elicits their long-lasting activation, which consistently becomes pyloric timed (Blitz et al., 2008). The ionic current(s) activated by CabTRP Ia in MCN1, CPN2, and AB_{CoG} remain to be determined. However, in crab STG neurons, this neuropeptide causes a long-lasting and selective activation of I_{MI} (modulator-activated, voltage-dependent inward current) in its targets (Golowasch and Marder, 1992; Swensen and Marder, 2000; DeLong et al., 2009a). Recent work in the crab STG similarly showed that bath applied proctolin, another I_{MI}-activating peptide, modulates transmitter release in a pyloric circuit neuron (Zhao et al., 2011). However, although proctolin does activate I_{MI} in the studied neuron (Golowasch and Marder, 1992; Swensen and Marder, 2000), it was not determined whether I_{MI} activation mediated the change in transmitter release (Zhao et al., 2011).

Direct modulation of descending projection neuron activity is established in several rhythmic motor systems (Blitz and Nusbaum, 1997; Dickinson et al., 1997; Le Ray et al., 2004; Crisp and Mesce, 2006; Blitz et al., 2008; Li et al., 2010). Modulatory actions also indirectly influence the excitability and activity pattern of these projection neurons by acting on inputs to them (Le Ray et al., 2004; Antri et al., 2008; Blitz and Nusbaum, 2008; DeLong et al., 2009a; Smetana et al., 2010; Nusbaum and Blitz, 2012). Some of these indirect modulatory actions occur at the presynaptic terminals of sensory inputs (Le Ray et al., 2004; Antri et al., 2008; Barrière et al., 2008). The POC modulation of AB feedback to MCN1 and CPN2 appears to be the first example of a presynaptic modulation of CPG feedback synapses.

Presynaptic regulation of synaptic actions is prevalent throughout all systems (Rossignol et al., 2006; Pelkey and McBain, 2007; Di and Tasker, 2008; Pinheiro and Mulle, 2008; Rudomin, 2009; Nusbaum and Blitz, 2012; Wang, 2012). Less is known about the circuit-level consequences resulting specifically from presynaptic modulation. Recent work in the first-stage olfactory microcircuit (olfactory bulb/antennal lobe) has revealed several examples of presynaptic modulation and its behavioral consequences (Ignell et al., 2009; Chalasani et al., 2010; Lepousez et al., 2010; Tobin et al., 2010; Root et al., 2011; Nusbaum and Blitz, 2012; Wang, 2012). Several circuit-level consequences of presynaptic modulation are also established in the vertebrate spinal locomotion system. For example, presynaptic modulation regulates the strength of sensory input onto the reticulospinal neurons (RSNs) that drive the spinal locomotor CPG (Le Ray et al., 2004, 2010; Antri et al., 2008). Within the spinal cord, several different signaling molecules modulate neurotransmitter release and thereby locally control the excitability of the locomotor CPG (Takahashi and Alford, 2002; Schwartz et al., 2005; Kyriakatos and El Manira, 2007; Chapman et al., 2008; Kyriakatos et al., 2009). Similarly, in several smaller motor systems, presynaptic modulation regulates sensory feedback to a CPG, CPG-generated motor patterns, and/or corollary discharge from a CPG (Chiel et al., 1988; DeLong et al., 2009b; Sakurai and Katz, 2009; Harris-Warrick and Johnson, 2010; Zhao et al., 2011).

One general advantage of presynaptic regulation is that it selectively targets a subset of the synapses made by a particular neuron. The AB neuron, for example, acts within the STG as the pyloric pacemaker neuron and as a gastric mill CPG neuron (Selverston and Miller, 1980; Hooper and Marder, 1987; Bartos et al., 1999; Saideman et al., 2007; White and Nusbaum, 2011), while within the CoGs it provides pyloric-timed feedback regulation to projection neurons (Blitz and Nusbaum, 2008; this study). The POC modulation of the AB feedback in the CoGs leaves the AB synapses within the STG unmodified (Fig. 9). Similarly, the mechanosensory ventral cardiac neurons (VCNs) trigger a distinct gastric mill motor pattern by a long-lasting

excitation of MCN1 and CPN2 plus a gastric mill protractor phase-specific presynaptic inhibition of AB_{CoG} synapses, which does not alter AB_{STG} synapses (Beenhakker and Nusbaum, 2004; Blitz and Nusbaum, 2008). In this latter case, the presynaptic inhibition appears to be mediated by a VCN-activated CoG neuron that is inhibited during the gastric mill retractor phase. Thus, the POC and VCN pathways trigger distinct gastric mill motor patterns largely as a result of their distinct (i.e., persistent vs phasic) regulation of AB_{CoG}, despite their shared activation of the same two projection neurons and lack of direct actions on the CPG neurons.

Our results support the hypothesis that all AB synapses in the CoG are modulated by POC activity, given that the AB synapses were also enhanced in projection neurons whose activity is not altered by POC stimulation. This is not a surprising result given that this POC action is likely mediated by its release of a neuropeptide [CabTRP Ia (Blitz et al., 2008)] and that neuropeptides commonly diffuse relatively long distances from their release sites to influence their target neurons (Jan and Jan, 1982; Nusbaum, 2002; Nässel and Winther, 2010).

CPG feedback to its projection neuron inputs is prevalent in many rhythmic motor systems (Gillette et al., 1978; Arshavsky et al., 1988; Dubuc and Grillner, 1989; Nagy et al., 1994; Frost and Katz, 1996; Norris et al., 1996; Ezure and Tanaka, 1997; Buchanan and Einum, 2008). One shared consequence of this feedback is to impose onto the projection neurons a rhythmic activity pattern that is time-locked to the CPG-driven motor pattern. However, only a few studies have established functional consequences for CPG-timed projection neuron activity. One such consequence is to prolong RSN activity, and hence that of the spinal locomotor CPG (Antri et al., 2009). Rhythmic CPG feedback has also been proposed to function as a phase-specific gate for sensory and/or higher-order inputs (Deliagina et al., 2000; Pflieger and Dubuc, 2004). In the crab STNS, CPG feedback regulates intercircuit interactions. For example, the pyloric CPG feedback to the projection neuron MCN1 entrains the gastric mill rhythm and regulates the gastric mill cycle period (Nadim et al., 1998; Bartos et al., 1999; Wood et al., 2004). In turn, gastric mill circuit feedback to the STG terminals of MCN1 results in a phase-specific regulation of the pyloric cycle period (Bartos and Nusbaum, 1997).

Intercircuit coordination occurs between many behaviors, such as locomotion and respiration (Gariépy et al., 2010). The coupling ratios between such coordinated motor patterns can change, and coordination can even be eliminated, although the associated cellular-level mechanisms are not fully elucidated (Bernasconi and Kohl, 1993; Clemens et al., 1998; Saunders et al., 2004; Gariépy et al., 2010, 2012). Our finding that the strength of the AB synapses onto projection neurons is flexible, and that these synapses contribute to intercircuit coordination, provides a potential general mechanism for plasticity during such events. One candidate locus in the vertebrate CNS for intercircuit coordination is the brainstem, where neurons in the lateral reticular nucleus exhibit activity that is coordinately time-locked to the respiration and locomotion motor patterns (Ezure and Tanaka, 1997), and respiratory neurons receive input from a subset of the mesencephalic locomotor region neurons that drive locomotion (Gariépy et al., 2012). Thus, coordination events in other systems may well also be mediated by CPG feedback, which may be a locus for the modulation of coordinated movements during complex behavior.

References

Antri M, Auclair F, Albrecht J, Djeudjang N, Dubuc R (2008) Serotoninergic modulation of sensory transmission to brainstem reticulospinal cells. Eur J Neurosci 28:655–667.

Antri M, Fénelon K, Dubuc R (2009) The contribution of synaptic inputs to sustained depolarizations in reticulospinal neurons. J Neurosci 29:1140–1151.

Arshavsky YI, Orlovsky GN, Perret C (1988) Activity of rubrospinal neurons during locomotion and scratching in the cat. Behav Brain Res 28:193–199.

Barrière G, Simmers J, Combes D (2008) Multiple mechanisms for integrating proprioceptive inputs that converge on the same motor pattern-generating network. J Neurosci 28:8810–8820.

Bartos M, Nusbaum MP (1997) Intercircuit control of motor pattern modulation by presynaptic inhibition. J Neurosci 17:2247–2256.

Bartos M, Manor Y, Nadim F, Marder E, Nusbaum MP (1999) Coordination of fast and slow rhythmic neuronal circuits. J Neurosci 19:6650–6660.

Beenhakker MP, Nusbaum MP (2004) Mechanosensory activation of a motor circuit by coactivation of two projection neurons. J Neurosci 24:6741–6750.

Beenhakker MP, Blitz DM, Nusbaum MP (2004) Long-lasting activation of rhythmic neuronal activity by a novel mechanosensory system in the crustacean stomatogastric nervous system. J Neurophysiol 91:78–91.

Bernasconi P, Kohl J (1993) Analysis of co-ordination between breathing and exercise rhythms in man. J Physiol 471:693–706.

Blitz DM, Nusbaum MP (1997) Motor pattern selection via inhibition of parallel pathways. J Neurosci 17:4965–4975.

Blitz DM, Nusbaum MP (1999) Distinct functions for cotransmitters mediating motor pattern selection. J Neurosci 19:6774–6783.

Blitz DM, Nusbaum MP (2008) State-dependent presynaptic inhibition regulates central pattern generator feedback to descending inputs. J Neurosci 28:9564–9574.

Blitz DM, Christie AE, Coleman MJ, Norris BJ, Marder E, Nusbaum MP (1999) Different proctolin neurons elicit distinct motor patterns from a multifunctional neuronal network. J Neurosci 19:5449–5463.

Blitz DM, Beenhakker MP, Nusbaum MP (2004) Different sensory systems share projection neurons but elicit distinct motor patterns. J Neurosci 24:11381–11390.

Blitz DM, White RS, Saideman SR, Cook A, Christie AE, Nadim F, Nusbaum MP (2008) A newly identified extrinsic input triggers a distinct gastric mill rhythm via activation of modulatory projection neurons. J Exp Biol 211:1000–1011.

Bonjean M, Baker T, Lemieux M, Timofeev I, Sejnowski T, Bazhenov M (2011) Corticothalamic feedback controls sleep spindle duration *in vivo*. J Neurosci 31:9124–9134.

Briggs F, Usrey WM (2008) Emerging views of corticothalamic function. Curr Opin Neurobiol 18:403–407.

Buchanan JT, Einum JF (2008) The spinobulbar system in lamprey. Brain Res Rev 57:37–45.

Bucher D, Taylor AL, Marder E (2006) Central pattern generating neurons simultaneously express fast and slow rhythmic activities in the stomatogastric ganglion. J Neurophysiol 95:3617–3632.

Chalasani SH, Kato S, Albrecht DR, Nakagawa T, Abbott LF, Bargmann CI (2010) Neuropeptide feedback modifies odor-evoked dynamics in *Caenorhabditis elegans* olfactory neurons. Nat Neurosci 13:615–621.

Chapman RJ, Issberner JP, Sillar KT (2008) Group I mGluRs increase locomotor network excitability in *Xenopus* tadpoles via presynaptic inhibition of glycinergic neurotransmission. Eur J Neurosci 28:903–913.

Chiel HJ, Kupfermann I, Weiss KR (1988) An identified histaminergic neuron can modulate the outputs of buccal-cerebral interneurons in *Aplysia* via presynaptic inhibition. J Neurosci 8:49–63.

Christie AE, Stein W, Quinlan JE, Beenhakker MP, Marder E, Nusbaum MP (2004) Actions of a histaminergic/peptidergic projection neuron on rhythmic motor patterns in the stomatogastric nervous system of the crab *Cancer borealis*. J Comp Neurol 469:153–169.

Clemens S, Massabuau JC, Legeay A, Meyrand P, Simmers J (1998) *In vivo* modulation of interacting central pattern generators in lobster stomatogastric ganglion: influence of feeding and partial pressure of oxygen. J Neurosci 18:2788–2799.

Coleman MJ, Nusbaum MP (1994) Functional consequences of compartmentalization of synaptic input. J Neurosci 14:6544–6552.

Crisp KM, Mesce KA (2006) Beyond the central pattern generator: amine modulation of decision-making neural pathways descending from the brain of the medicinal leech. J Exp Biol 209:1746–1756.

Deliagina TG, Zelenin PV, Fagerstedt P, Grillner S, Orlovsky GN (2000) Activity of reticulospinal neurons during locomotion in the freely behaving lamprey. J Neurophysiol 83:853–863.

DeLong ND, Kirby MS, Blitz DM, Nusbaum MP (2009a) Parallel regulation of a modulator-activated current via distinct dynamics underlies comodulation of motor circuit output. J Neurosci 29:12355–12367.

DeLong ND, Beenhakker MP, Nusbaum MP (2009b) Presynaptic inhibition selectively weakens peptidergic cotransmission in a small motor system. J Neurophysiol 102:3492–3504.

Di S, Tasker JG (2008) Rapid synapse-specific regulation of hypothalamic magnocellular neurons by glucocorticoids. Prog Brain Res 170:379–388.

Dickinson PS (2006) Neuromodulation of central pattern generators in invertebrates and vertebrates. Curr Opin Neurobiol 16:604–614.

Dickinson PS, Fairfield WP, Hetling JR, Hauptman J (1997) Neurotransmitter interactions in the stomatogastric system of the spiny lobster: one peptide alters the response of a central pattern generator to a second peptide. J Neurophysiol 77:599–610.

Doi A, Ramirez JM (2008) Neuromodulation and the orchestration of the respiratory rhythm. Respir Physiol Neurobiol 164:96–104.

Dubuc R, Grillner S (1989) The role of spinal cord inputs in modulating the activity of reticulospinal neurons during fictive locomotion in the lamprey. Brain Res 483:196–200.

Ego-Stengel V, Le Cam J, Shulz DE (2012) Coding of apparent motion in the thalamic nucleus of the rat vibrissal somatosensory system. J Neurosci 32:3339–3351.

Eisen JS, Marder E (1982) Mechanisms underlying pattern generation in lobster stomatogastric ganglion as determined by selective inactivation of identified neurons. III. Synaptic connections of electrically coupled pyloric neurons. J Neurophysiol 48:1392–1415.

Ezure K, Tanaka I (1997) Convergence of central respiratory and locomotor rhythms onto single neurons of the lateral reticular nucleus. Exp Brain Res 113:230–242.

Frost WN, Katz PS (1996) Single neuron control over a complex motor program. Proc Natl Acad Sci U S A 93:422–426.

Gariépy JF, Missaghi K, Dubuc R (2010) The interactions between locomotion and respiration. Prog Brain Res 187:173–188.

Gariépy JF, Missaghi K, Chevallier S, Chartré S, Robert M, Auclair F, Lund JP, Dubuc R (2012) Specific neural substrate linking respiration to locomotion. Proc Natl Acad Sci U S A 109:E84–E92.

Gillette R, Kovac MP, Davis WJ (1978) Command neurons in *Pleurobranchaea* receive synaptic feedback from the motor network they excite. Science 199:798–801.

Golowasch J, Marder E (1992) Proctolin activates an inward current whose voltage dependence is modified by extracellular Ca^{2+}. J Neurosci 12:810–817.

Gutierrez GJ, Grashow RG (2009) *Cancer borealis* stomatogastric nervous system dissection. J Vis Exp 25:pii:1207.

Harris-Warrick RM, Johnson BR (2010) Checks and balances in neuromodulation. Front Behav Neurosci 4:pii:47.

Hedrich UB, Diehl F, Stein W (2011) Gastric and pyloric motor pattern control by a modulatory projection neuron in the intact crab, *Cancer pagurus.* J Neurophysiol 105:1671–1680.

Heinzel HG, Weimann JM, Marder E (1993) The behavioral repertoire of the gastric mill in the crab, *Cancer pagurus*: an *in situ* endoscopic and electrophysiological examination. J Neurosci 13:1793–1803.

Hooper SL, Marder E (1987) Modulation of the lobster pyloric rhythm by the peptide proctolin. J Neurosci 7:2097–2112.

Ignell R, Root CM, Birse RT, Wang JW, Nässel DR, Winther AM (2009) Presynaptic peptidergic modulation of olfactory receptor neurons in *Drosophila.* Proc Natl Acad Sci U S A 106:13070–13075.

Jan LY, Jan YN (1982) Peptidergic transmission in sympathetic ganglia of the frog. J Physiol 327:219–246.

Jordan LM, Sławińska U (2011) Chapter 12—Modulation of rhythmic movement: control of coordination. Prog Brain Res 188:181–195.

Kyriakatos A, El Manira A (2007) Long-term plasticity of the spinal locomotor circuitry mediated by endocannabinoid and nitric oxide signaling. J Neurosci 27:12664–12674.

Kyriakatos A, Molinari M, Mahmood R, Grillner S, Sillar KT, El Manira A (2009) Nitric oxide potentiation of locomotor activity in the spinal cord of the lamprey. J Neurosci 29:13283–13291.

Lepousez G, Mouret A, Loudes C, Epelbaum J, Viollet C (2010) Somatostatin contributes to in vivo gamma oscillation modulation and odor discrimination in the olfactory bulb. J Neurosci 30:870–875.

Le Ray D, Brocard F, Dubuc R (2004) Muscarinic modulation of the trigemino-reticular pathway in lampreys. J Neurophysiol 92:926–938.

Le Ray D, Juvin L, Boutin T, Auclair F, Dubuc R (2010) A neuronal substrate for a state-dependent modulation of sensory inputs in the brainstem. Eur J Neurosci 32:53–59.

Li WC, Roberts A, Soffe SR (2010) Specific brainstem neurons switch each other into pacemaker mode to drive movement by activating NMDA receptors. J Neurosci 30:16609–16620.

Marder E, Bucher D (2007) Understanding circuit dynamics using the stomatogastric nervous system of lobsters and crabs. Annu Rev Physiol 69:291–316.

Marder E, Eisen JS (1984a) Transmitter identification of pyloric neurons: electrically coupled neurons use different transmitters. J Neurophysiol 51:1345–1361.

Marder E, Eisen JS (1984b) Electrically coupled pacemaker neurons respond differently to same physiological inputs and neurotransmitters. J Neurophysiol 51:1362–1374.

Miller JP, Selverston AI (1982a) Mechanisms underlying pattern generation in lobster stomatogastric ganglion as determined by selective inactivation of identified neurons. II. Oscillatory properties of pyloric neurons. J Neurophysiol 48:1378–1391.

Miller JP, Selverston AI (1982b) Mechanisms underlying pattern generation in lobster stomatogastric ganglion as determined by selective inactivation of identified neurons. IV. Network properties of pyloric system. J Neurophysiol 48:1416–1432.

Nadim F, Manor Y, Nusbaum MP, Marder E (1998) Frequency regulation of a slow rhythm by a fast periodic input. J Neurosci 18:5053–5067.

Nagy F, Cardi P, Cournil I (1994) A rhythmic modulatory gating system in the stomatogastric nervous system of *Homarus gammarus.* I. Pyloric-related neurons in the commissural ganglia. J Neurophysiol 71:2477–2489.

Nässel DR, Winther AM (2010) *Drosophila* neuropeptides in regulation of physiology and behavior. Prog Neurobiol 92:42–104.

Norris BJ, Coleman MJ, Nusbaum MP (1994) Recruitment of a projection neuron determines gastric mill motor pattern selection in the stomatogastric nervous system of the crab, *Cancer borealis.* J Neurophysiol 72:1451–1463.

Norris BJ, Coleman MJ, Nusbaum MP (1996) Pyloric motor pattern modification by a newly identified projection neuron in the crab stomatogastric nervous system. J Neurophysiol 75:97–108.

Nusbaum MP (2002) Regulating peptidergic modulation of rhythmically active neural circuits. Brain Behav Evol 60:378–387.

Nusbaum MP, Blitz DM (2012) Neuropeptide modulation of microcircuits. Curr Opin Neurobiol. Advance online publication. doi: 10.1016/j.conb.2012.01.003.

Pelkey KA, McBain CJ (2007) Differential regulation at functionally divergent release sites along a common axon. Curr Opin Neurobiol 17:366–373.

Pflieger JF, Dubuc R (2004) Vestibulo-reticular projections in adult lamprey: their role in locomotion. Neuroscience 129:817–829.

Pinheiro PS, Mulle C (2008) Presynaptic glutamate receptors: physiological functions and mechanisms of action. Nat Rev Neurosci 9:423–436.

Root CM, Ko KI, Jafari A, Wang JW (2011) Presynaptic facilitation by neuropeptide signaling mediates odor-driven food search. Cell 145:133–144.

Rossignol S, Dubuc R, Gossard JP (2006) Dynamic sensorimotor interactions in locomotion. Physiol Rev 86:89–154.

Rudomin P (2009) In search of lost presynaptic inhibition. Exp Brain Res 196:139–151.

Saideman SR, Blitz DM, Nusbaum MP (2007) Convergent motor patterns from divergent circuits. J Neurosci 27:6664–6674.

Sakurai A, Katz PS (2009) State-, timing-, and pattern-dependent neuromodulation of synaptic strength by a serotonergic interneuron. J Neurosci 29:268–279.

Saunders SW, Rath D, Hodges PW (2004) Postural and respiratory activation of the trunk muscles changes with mode and speed of locomotion. Gait Posture 20:280–290.

Schwartz EJ, Gerachshenko T, Alford S (2005) 5-HT prolongs ventral root

bursting via presynaptic inhibition of synaptic activity during fictive locomotion in lamprey. J Neurophysiol 93:980–988.
Selverston AI, Miller JP (1980) Mechanisms underlying pattern generation in lobster stomatogastric ganglion as determined by selective inactivation of identified neurons. I. Pyloric system. J Neurophysiol 44:1102–1121.
Sillito AM, Cudeiro J, Jones HE (2006) Always returning: feedback and sensory processing in visual cortex and thalamus. Trends Neurosci 29:307–316.
Smetana R, Juvin L, Dubuc R, Alford S (2010) A parallel cholinergic brainstem pathway for enhancing locomotor drive. Nat Neurosci 13:731–738.
Swensen AM, Marder E (2000) Multiple peptides converge to activate the same voltage-dependent current in a central pattern-generating circuit. J Neurosci 20:6752–6759.
Takahashi M, Alford S (2002) The requirement of presynaptic metabotropic glutamate receptors for the maintenance of locomotion. J Neurosci 22:3692–3699.
Tobin VA, Hashimoto H, Wacker DW, Takayanagi Y, Langnaese K, Caquineau C, Noack J, Landgraf R, Onaka T, Leng G, Meddle SL, Engelmann M, Ludwig M (2010) An intrinsic vasopressin system in the olfactory bulb is involved in social recognition. Nature 464:413–417.
Wang JW (2012) Presynaptic modulation of early olfactory processing in *Drosophila.* Dev Neurobiol 72:87–99.
Weimann JM, Meyrand P, Marder E (1991) Neurons that form multiple pattern generators: identification and multiple activity patterns of gastric/pyloric neurons in the crab stomatogastric system. J Neurophysiol 65:111–122.
White RS, Nusbaum MP (2011) The same core rhythm generator underlies different rhythmic motor patterns. J Neurosci 31:11484–11494.
Wood DE, Manor Y, Nadim F, Nusbaum MP (2004) Intercircuit control via rhythmic regulation of projection neuron activity. J Neurosci 24:7455–7463.
Zhao S, Sheibanie AF, Oh M, Rabbah P, Nadim F (2011) Peptide neuromodulation of synaptic dynamics in an oscillatory network. J Neurosci 31:13991–14004.